



1

2

3

4 **Dynamics and environmental drivers of methane and nitrous oxide fluxes at**
5 **the soil and ecosystem levels in a wet tropical forest**

6

7 **Authors**

8 Laëtitia M. Bréchet¹, Mercedes Ibáñez¹, Robert B. Jackson², Benoît Burban¹, Clément Stahl¹, Damien
9 Bonai³, Ivan A. Janssens⁴

10

11 ¹INRAE, UMR EcoFoG, CNRS, Cirad, AgroParisTech, Université des Antilles, Université de Guyane,
12 Kourou, FR-97310, France

13 ²Department of Earth System Science, Woods Institute for the Environment, and Precourt Institute for
14 Energy, Stanford University, Stanford, CA 94305-2210, USA

15 ³Université de Lorraine, AgroParisTech, INRAE, UMR Silva, Nancy, FR-54000, France

16 ⁴Research Group Plant and Ecosystems (PLECO), Department of Biology, University of Antwerp, Wilrijk,
17 BE-2610, Belgium

18

19 **Correspondence:** Laëtitia M. Bréchet (laeti.brechet@gmail.com)

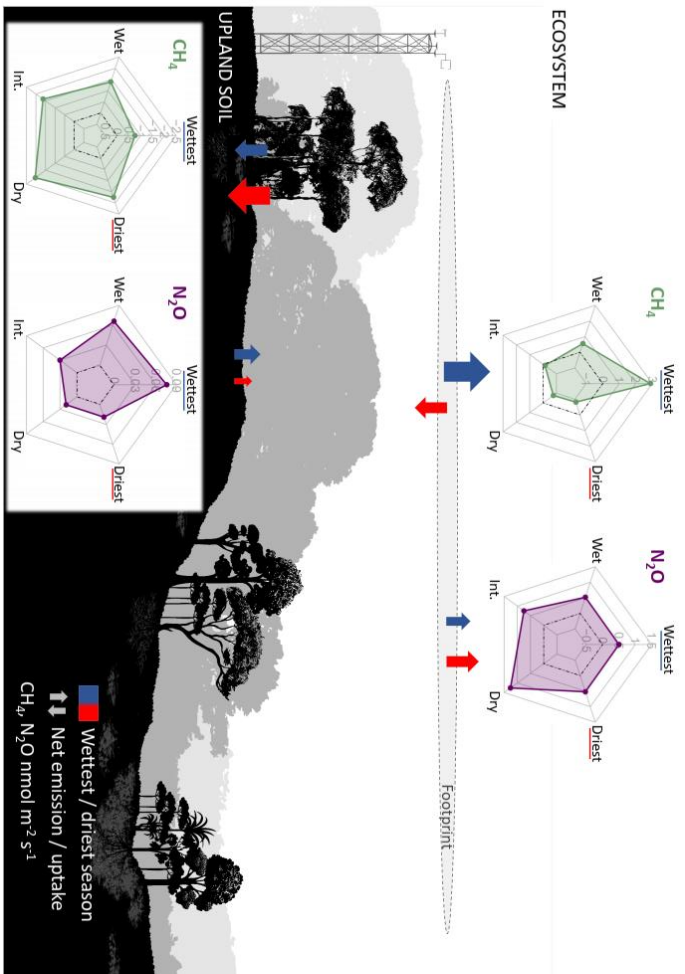
20

21 **Abstract**

22 Tropical forests are critical for maintaining the global carbon balance and mitigating climate change,
23 yet their exchange of greenhouse gases with the atmosphere remains understudied, particularly for
24 methane (CH₄) and nitrous oxide (N₂O). This study reports on continuous measurements of CH₄ and
25 N₂O fluxes at the ecosystem and soil levels, respectively through eddy covariance and an automated



26 chamber technique, in a wet tropical forest in French Guiana over a period of 26 months. We studied
27 the magnitude of CH₄ and N₂O fluxes and their drivers (climatic variables) during two extreme periods,
28 the driest and wettest seasons. Seasonal ecosystem fluxes showed near-zero net CH₄ uptake during
29 the driest season and emissions occurring during the wettest season that were larger in magnitude
30 than the uptake. Meanwhile, N₂O emissions were of similar magnitudes in both seasons. Some upland
31 soils within the footprint of the eddy covariance tower emitted N₂O in both seasons, although these
32 fluxes were particularly small. None of the measured climatic variables could explain this soil N₂O flux
33 variation. In contrast, the upland soils were characterised by CH₄ uptake. Overall, seasonal ecosystem
34 CH₄ and N₂O fluxes, as well as seasonal upland soil CH₄ fluxes, were partially explained by seasonal
35 variations in soil water content and global radiation. In addition to the upland soil fluxes studied, the
36 magnitude and sign of the net ecosystem fluxes of CH₄ and N₂O were likely due to outgassing from
37 aboveground biomass and the presence of seasonally flooded areas within the footprint of the eddy
38 covariance system. Further studies of other ecosystem compartments in different forest habitats are
39 needed to better understand the temporal variations in CH₄ and N₂O fluxes in wet tropical forests.



The 26-month study in a wet tropical forest revealed seasonal CH₄ and N₂O fluxes at the ecosystem and soil levels. Daily means of CH₄ and N₂O fluxes were highly variable, changing direction and magnitude on short time scales.





1 Introduction

The lack of knowledge on greenhouse gas fluxes in the tropical forests of the Amazon Basin contributes significantly to the uncertainty in the global greenhouse gas budget, particularly for methane (CH_4) and nitrous oxide (N_2O) (Davidson et al., 2012; Covey et al., 2021), the two most important greenhouse gases in the atmosphere after carbon dioxide (CO_2). Early observations show that tropical forests in the Amazon Basin may contribute disproportionately to global CH_4 and N_2O exchanges compared to other forests (Tian et al., 2015), but considerable uncertainties remain due to the paucity of data and lack of detailed understanding of CH_4 and N_2O cycling at both soil and ecosystem levels in these forests. The role of tropical forest soils is crucial here as they can act either as a source or a sink for CH_4 and N_2O (Bouwman et al., 1993). In contrast to the consistent emissions from soil microbial decomposition and root activity for CO_2 , anaerobic CH_4 -emitting microbes (methanogenic archaea) are dominant in wetland environments, whereas aerobic CH_4 -consuming microbes (methanotrophic bacteria) are more abundant in upland soils (Ito and Inatomi, 2012; Welch et al., 2019) where they play the role of CH_4 sinks. For N_2O as well, both emission and uptake can occur in soils. N_2O can be produced by microbes under both anaerobic (via denitrification) and aerobic (via nitrification) conditions (Khalil et al., 2004), although the majority of N_2O production occurs in waterlogged soils (Oertel et al., 2016). On the other hand, soil microbes that are not denitrifiers can reduce N_2O to dinitrogen (Sanford et al., 2012; Jones et al., 2014).

Microbial CH_4 and N_2O fluxes in tropical soils are controlled by the complex interplay of multiple environmental and biological factors. The key factors regulating net CH_4 fluxes in tropical soils include redox potential and water table depth (Silver et al., 1999; Teh et al., 2005; von Fischer and Hedin, 2007), plant productivity (Whiting and Chanton, 1993; von Fischer and Hedin, 2007), labile soil organic matter (Wright et al., 2011), competition for carbon substrates among anaerobic microorganisms (Teh and Silver, 2006; von Fischer and Hedin, 2007), temperature (Knox et al., 2021), and the presence of plants that facilitate atmospheric escape (Pangala et al., 2013). The key factors regulating net soil N_2O fluxes in tropical soils include redox potential, soil water content (SWC) or water table depth,



67 temperature, pH, labile carbon availability and labile nitrogen availability (Groffman et al., 2009). For
68 both CH₄ and N₂O flux dynamics, of all these factors, variations in soil redox conditions, mediated by
69 variations in water table depth, play a particularly important regulatory role in tropical soils (Zhu et al.,
70 2013; Yu et al., 2021) due to the underlying physiology of the microbes that produce and uptake CH₄
71 and N₂O.

72 Production and uptake of both CH₄ and N₂O in the soil are highly variable in space (hot spots) and time
73 (hot moments) (Blagodatsky and Smith, 2012). This is because microbial processes are discontinuous
74 (Blagodatsky and Smith, 2012), environmental conditions can change rapidly at short timescales, and
75 the strong seasonality of climate conditions, with pronounced wet and dry seasons, in most tropical
76 forests can significantly affect physical and ecophysiological ecosystem processes, which in turn affect
77 greenhouse gas fluxes. In addition, most published N₂O and CH₄ flux data from tropical ecosystems
78 have been derived from chamber-based measurements at the soil level, often with low spatial and
79 temporal resolutions. Automated soil chambers capture fine-scale temporal variations, including hot
80 moments. However, they represent only a tiny part of the landscape (i.e. a few square metres of soil
81 surface at most) and therefore fail to capture emergent ecosystem properties that may be manifest at
82 larger spatial scales. Moreover, above-ground plant tissues also exchange CH₄ and N₂O with the
83 atmosphere (i.e. produced in the soil and transported in the transpiration stream and/or by diffusion,
84 or produced within the stems), and this cannot be captured by soil chamber measurements alone. This
85 makes chamber approaches insufficient to quantify the magnitude and seasonal pattern of whole-
86 ecosystem greenhouse gas fluxes. Chamber-based measurements also hamper our ability to assess the
87 role of tropical forests in the exchange of CH₄ and N₂O between the atmosphere and the land surface,
88 and induce large uncertainties in our current assessment of the greenhouse gas sink potential of
89 tropical forests.

90 On the other hand, a combination of soil and ecosystem level measurements can be a powerful tool
91 to reduce the gap between different levels of measurement (e.g. plot to ecosystem) (Lucas-Moffat et
92 al., 2018). Continuous ecosystem-level measurements via the eddy covariance technique provide high



temporal resolution data on mass and energy exchanges at the ecosystem level (Baldocchi, 2014, 2020; Delwiche et al., 2021) and more detailed information on ecosystem functioning at a broader spatial scale than do mere soil measurements, which miss above-ground exchanges and typically, also emissions from wetland areas within the ecosystem (Bonal et al., 2008; Aguilos et al., 2018; Wang et al., 2021; Liu et al., 2022). However, eddy covariance cannot indicate how much different land cover types relatively contribute to the ecosystem's total flux since the measurements integrate high and low frequency flows over time and space. Chamber and eddy covariance-based approaches each have their own strengths and weaknesses; however, taken together, they effectively represent the magnitude of ecosystem fluxes and can help determine the drivers of greenhouse gas flux dynamics (Eugster et al., 2015). We therefore combined these two approaches to test the following assumptions:

- H1: Ecosystem- and soil-level CH₄ and N₂O fluxes vary seasonally in the studied tropical forest, switching between uptake and emission,
- H2: At both the soil and ecosystem levels, SWC is the primary abiotic driver of these gaseous fluxes during the driest and wettest seasons.

This study provides, for the first time, a comprehensive assessment of CH₄ and N₂O dynamics at both ecosystem and soil levels based on high-frequency eddy covariance and continuous soil chamber time series over 26 months in a wet tropical forest.

2 Methods

2.1 Study site

Our research was conducted at the Guyaflux site (5°16'54"N, 52°54'44"W) (Bonal et al., 2008), an ICOS-associated ecosystem station (GF-Guy) located 15 km from the coast and approximately 40 km west of Kourou, in French Guiana, South America. On a decadal time scale, the average annual precipitation at the study site is 3102 ± 70 mm and average annual air temperature is 25.7 ± 0.1 °C (Aguilos et al., 2018). The climate is humid tropical and highly seasonal due to the north-south movement of the Inter-Tropical Convergence Zone (ITCZ), which drives regional precipitation. The ITCZ dictates the wet season



119 (from December to July, with rainfall of up to 500 mm month⁻¹) and the long dry season from mid-
120 August (mid-November, with less than 100 mm month⁻¹). In the northernmost part of the Guiana
121 shield, where the study site is located, the topography results in a succession of small elliptical hills
122 from 10 to 40 m asl, with soils classified as nutrient-poor acrisols (IUSS Working Group WRB, 2015).
123 The site is totally surrounded by undisturbed forest, locally characterised by a tree density of about
124 620 trees ha⁻¹ (for trees > 10 cm dbh), an average tree height of 35 m, an average tree diameter at
125 breast height (DBH) of 40.1 cm, with emergent trees over 40 m tall, and a tree species richness of about
126 140 species ha⁻¹ (Bonal et al., 2008; Aguilos et al., 2018; Daniel et al., 2023).

127

128 **2.2 Tower-based flux measurements**

129 Continuous measurements of the surface-atmosphere exchange of CO₂, H₂O and energy were initiated
130 in 2003 based on the Euroflux methodology (Aubinet et al., 2000) and the eddy covariance approach
131 (Baldocchi, 2003); they have previously been reported and fully documented (Bonal et al., 2008;
132 Aguilos et al., 2018). The Guyaflux flux tower is 55 m high and extends about 20 m beyond the top of
133 the canopy. The putative average footprint of the eddy fluxes from the tower covers approximately 50
134 - 100 ha of undisturbed forest in the direction of the prevailing winds (Bonal et al., 2008; Fang et al.,
135 2024). Within the estimated footprint of the Guyaflux tower, 52% of the area is upland forest, 13% is
136 seasonally flooded forest and the rest (35%) is slope forest (Fig. S1). Most of the meteorological and
137 eddy flux sensors are mounted three meters above the top of the tower, and include equipment
138 measuring air temperature and humidity (HMP155, Vaisala, Helsinki, Finland), bulk precipitation
139 (ARG100, EM Imt, Sunderland, UK), wind direction and speed (A05103-5, Young, Traverse City, MI,
140 USA), and global infrared incident and reflected radiation (R_g) (CNR1, Kipp and Zonen, Bohemia, NY,
141 USA). All the meteorological data in the present study were collected at 1-min intervals and compiled
142 as 30-min averages or sums with data loggers (CR23X, CR1000 or CR3000 models; Campbell Scientific
143 Inc., Utah, USA).



144 In 2017, a closed-path fast greenhouse gas analyser (FGGA, Los Gatos Research, Mountain View,
145 California, USA), whose head (gas inlet) was mounted 0.3 m from the head of a 3-D sonic anemometer
146 (R3-50; Gill Instruments, Lymington, UK), was set up at the top of the eddy flux tower to provide eddy
147 covariance measurements of the CH₄ and N₂O fluxes. The FGGA, equipped with a fourth-generation
148 cavity-enhanced laser absorption spectroscopy analyser (DLT-100; Los Gatos Research Inc.), was
149 connected to an external pump (Edwards XDS-35i, Edwards, England, UK) and to a 62 m long PFA inlet
150 tube (4 mm inlet diameter) protected by black foam with a 15 µm filter. All data were sampled at a
151 frequency of 20 Hz with data loggers (model CR3000; Campbell Scientific Inc.).
152 In addition, to take conditions where non-turbulent processes prevail (e.g. calm nights) into account,
153 the eddy covariance measurements were complemented with a vertical profile measurement system
154 to estimate variations in CH₄ and N₂O concentrations at six different heights (i.e. 0.5, 6, 13, 23, 32 and
155 58 m) with a 0.8 L min⁻¹ pump connected to a six-line solenoid valve and a closed-path FGGA (FGGA,
156 Los Gatos Research, Mountain View, California, USA). The entire system was controlled by a data logger
157 (model CR10X; Campbell Scientific Inc.), which recorded greenhouse gas concentration data every 15
158 min. The vertical profile system for CH₄ and N₂O was stopped after one year because the storage of
159 the gases was found to be negligible (see below).

160

161 **2.3 Tower-based CH₄ and N₂O flux computation**

162 We used EDDYPRO V6.2.2 (LI-COR Inc.), a software based on a set of standardised post-processing
163 calculations and corrections, to calculate CH₄ and N₂O fluxes from the raw high-frequency eddy
164 covariance data. The parameterization of the software included: a two-dimensional coordinate
165 rotation to set lateral and vertical mean wind speed to zero; a time lag between each scalar and wind
166 speed measurement estimated by covariance maximisation; an empirical frequency correction for
167 high-frequency attenuation; and a Webb-Pearman-Leuning correction for density fluctuations where
168 required, i.e. where concentrations were not measured as mixing ratios. Details of these corrections
169 are given in Aubinet et al. (2012). After the greenhouse gas flux computation, the EDDYPRO output



170 files contained continuous time series for ecosystem-atmosphere greenhouse gas (CH₄ and N₂O) fluxes
171 reported at a 30-min time step (from 17 May, 2016 to 2 August, 2018). The output files also included
172 uncertainties, quality control flags, friction velocity, and basic environmental and meteorological data.
173 To calculate net ecosystem production and uptake, we added the storage term to the turbulent flux
174 measured by the eddy covariance tower. This correction is particularly relevant for CO₂ exchanges in
175 forest ecosystems to reduce the uncertainty of the net flux estimate (Nicolini et al., 2018). However,
176 for the net CH₄ and N₂O fluxes, the relevance of the storage term correction was only marginal. In
177 contrast to CO₂, whose concentrations clearly built up at soil level during low-turbulence conditions,
178 this was not the case for N₂O and CH₄, and comparisons between the ecosystem fluxes with and
179 without correction for the storage term showed that the change in the resulting flux was minimal (Figs.
180 S2, S3). Consequently, we assumed that the storage of CH₄ and N₂O was negligible and ignored it in
181 this study. This meant that a larger period of eddy covariance flux measurements could be used
182 (starting in 2016), in addition to the January 2017 - January 2018 period where CH₄ and N₂O storage
183 data were available. Ecosystem fluxes of CH₄ and N₂O were calculated every half-hour (nmol m⁻² s⁻¹).
184

185 **2.4 Chamber measurements**

186 In addition to the flux tower and its associated instrumentation, automated static non-steady through-
187 flow chambers for continuous measurement of soil greenhouse gas fluxes were installed in June 2016
188 on hypoferralic soils with deep vertical drainage and a very deep water table (~15 m depth),
189 approximately 50 m upwind from the flux tower in some of the upland forest part of the tower
190 footprint (Fig. S1). This automated system had two constraints, which when combined, limited the
191 spatial coverage of the soil greenhouse gas flux measurements to the upland forest area: the power
192 supply was only available at the flux tower, and the maximum distance between the automated
193 chambers and the gas analysers was 30 m. Thirteen of the sixteen initial chambers functioned correctly
194 throughout the study period and their data were retained in this study. Briefly, the chambers (LI-8100-
195 104, LI-COR Inc., Lincoln, NE, USA) were mounted on PVC collars (20.3-cm inner diameter; enclosed



196 soil area $\sim 318 \text{ cm}^2$; offset $\sim 4 \text{ cm}$) that were permanently inserted into the soil. The chambers were
197 connected to a multiplexer (LI-8150, LI-COR Inc.), used to program specific measurement cycles, which
198 operated with a cavity ring-down spectroscopy (CRDS) analyser (G2308; Picarro Inc., Santa Clara, CA,
199 USA) to measure CO_2 , H_2O and dry air- CH_4 and N_2O concentrations (water corrected concentrations)
200 at 1 Hz. This analyser relied on an external recirculation pump (A0702; Picarro Inc.). The multiplexer
201 program purged the system 15 s before and 45 s after the measurements to flush out the tubing and
202 return to ambient-air greenhouse gas concentrations. A dead band of 60 s avoided potential
203 measurement errors ascribed to pressure changes inside the chamber-tubing-analyser loop following
204 chamber or solenoid valve closure and accounted for time lags. In addition, the program included two
205 different closure times to account for high and low fluxes, i.e. 2-min and 25-min measurement periods.
206 The equipment is described in more detail in previous publications (Courtois et al., 2019; Bréchet et
207 al., 2021).

208

209 **2.5 Chamber-based CH_4 and N_2O flux computation**

210 We used the SOILFLUXPRO software (LI-COR Biosciences) to compute soil greenhouse gas fluxes based
211 on the linear and exponential regression of the change in headspace concentrations over time, the
212 collar area and the system volume, after correction for atmospheric pressure and temperature. Flux
213 values were selected based on the model that provided the best fit and highest determination
214 coefficient (R^2).

215 After calculating the fluxes and implementing our standard soil greenhouse gas QC procedure (Courtois
216 et al., 2019; Bréchet et al., 2021), all CO_2 fluxes with an insufficiently high R^2 (< 0.90), an initial
217 concentration greater than 900 ppm, or a value outside the range of variation from 0.10 to $30 \mu\text{mol}$
218 $\text{m}^{-2} \text{ s}^{-1}$ were discarded for all three gases, based on the assumption that poor-quality CO_2 implied poor-
219 quality values for CH_4 and N_2O . As an improvement over Courtois et al. (2019), all CH_4 fluxes with $R^2 <$
220 0.80 were excluded regardless of the measurement length (i.e. 2-min and 25-min). For N_2O , all short
221 measurements (i.e. 2-min) with $R^2 < 0.80$ were discarded. In addition, based on the metric proposed



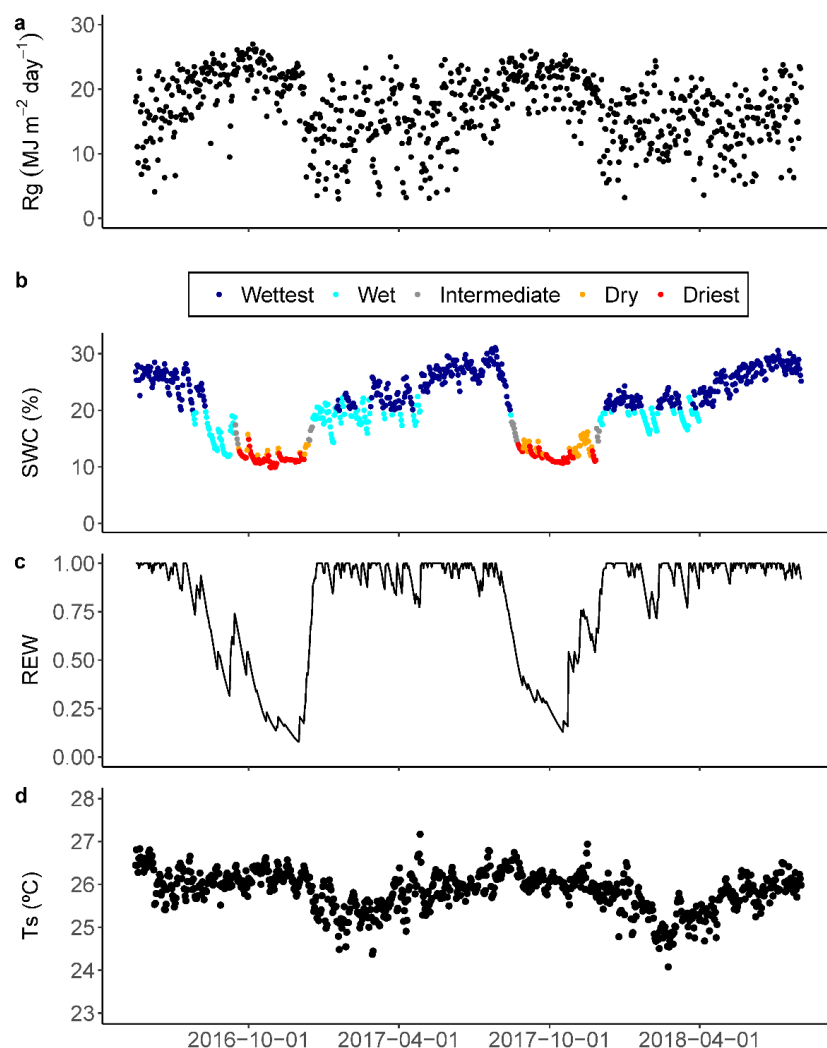
222 by Nickerson (2016), we calculated minimum detectable fluxes suitable for high-resolution in situ
223 greenhouse gas measurements as $0.040 \text{ nmol m}^{-2} \text{ s}^{-1}$ and $0.002 \text{ nmol m}^{-2} \text{ s}^{-1}$ for 2 min and 25 min
224 respectively for CH_4 and $0.100 \text{ nmol m}^{-2} \text{ s}^{-1}$ and $0.002 \text{ nmol m}^{-2} \text{ s}^{-1}$ for 2 min and 25 min respectively for
225 N_2O . The soil fluxes of CH_4 and N_2O ($\text{nmol m}^{-2} \text{ s}^{-1}$) were then assigned to the respective half-hours.

226

227 **2.6 Tower and chamber flux data analysis**

228 In order to include the most complete information possible, we based the study period on the soil flux
229 measurements and included all available data from 17 May, 2016 to 2 August, 2018. This 26-month
230 period included both very dry and very wet seasons (Fig. 1).

231



232

233 Figure 1. Daily (a) accumulated global radiation (Rg); (b) average soil water content (SWC) at 5 cm in
 234 depth during the wet, intermediate and dry seasons, and for two contrasted seasons defined as the
 235 wettest (dark blue dots) and the driest (red dots); (c) average relative extractable water (REW) to 3 m
 236 in depth based on the water balance model developed by Wagner et al. (2011); and (d) soil
 237 temperature (Ts) at 5 cm in depth, from 17 May, 2016 to 2 August, 2018 in the Guyaflux tropical forest,
 238 French Guiana. See Sect. 2.7 for details of the methods used to define the “driest” and “wettest”
 239 periods with extreme SWC.



240 Some flawed data was found (and eliminated) for both eddy covariance and soil chamber
241 measurements. They resulted from particular physical or biological conditions at the sampling point or
242 inside the soil chamber (e.g. wasp nests, disturbance by birds, dust, a branch preventing proper closure
243 of the chamber and causing a leak), or from mechanical issues (e.g. a power cut, soil chamber
244 remaining closed, gas analyser malfunction), which generated gaps in each time series. After flux
245 computation, the eddy covariance data for CH₄ and N₂O were filtered: data below a u^* threshold of
246 0.15 m s^{-1} were discarded (Bonal et al., 2008) - as were data with a quality flag of 2 (on a scale from 0
247 to 2) (Mauder and Foken, 2004).

248 For eddy covariance and chamber data, the 30 min observations were filtered and flux values outside
249 the 5th - 95th percentile flux range were discarded. To calculate daily averages for greenhouse gas
250 fluxes, we first estimated the optimal number of observations per day necessary to obtain
251 representative daily averages. To do this, we selected a data pool with at least 42 observations per day
252 in the eddy covariance dataset. In the soil chamber dataset, we calculated daily means for each of the
253 thirteen chambers and retained only the data when at least five observations per chamber per day
254 were recorded. Subsets of values from 1 to 42 for the eddy covariance data and from 1 to 13 for the
255 soil chamber data were then created for each day based on 100 bootstrap iterations. Representative
256 daily means were found for thresholds of 12 minimum observations per day for eddy covariance and
257 10 for chamber data. These tests were performed separately for CH₄ and N₂O and the driest and
258 wettest seasons, giving similar threshold results. Daily means with a number of observations below the
259 corresponding threshold were then discarded from further analyses. After filtering out the non-
260 representative days, the missing daily means for the whole study period represented 27% for both CH₄
261 and N₂O flux data derived from eddy covariance, and 34% and 30%, respectively, for CH₄ and N₂O flux
262 data derived from the soil chambers.

263



264 **2.7 Environmental measurements**

265 In the vicinity of the tower, we used temperature sensors (CS107; Campbell Scientific Inc., Logan, UT,
266 USA) to measure surface soil temperature (T_s) and frequency domain sensors (CS615 or CS616;
267 Campbell Scientific Inc.) to measure soil volumetric water content (SWC) at a depth of 5 cm. To
268 estimate the daily relative extractable water (REW) for trees from the soil surface to a depth of 3 m,
269 we used a soil water balance model previously validated for tropical forests (Wagner et al., 2011), with
270 daily precipitation, evapotranspiration and solar radiation as input variables. Daily SWC (%), T_s (°C) and
271 REW were defined as the average of the half-hourly flux values over 24 h, while daily R_g ($\text{MJ m}^{-2} \text{ day}^{-1}$)
272 was the sum of the half-hourly flux values over 24 h.

273 To examine the effect of environmental variables on CH_4 and N_2O fluxes at the ecosystem and soil
274 levels, we extracted data from two contrasting periods, termed “Driest” and “Wettest” (Fig. 1). The
275 driest days occurred at the end of the dry season, when SWC was less than 15% and decreased for at
276 least three consecutive days. The wettest days had a SWC above 20%, corresponding to a REW above
277 0.4, and unlimited available water for trees (Wagner et al., 2011) for more than two consecutive days.

278

279 **2.8 Data analysis**

280 We used the `mgcv` (Wood and Wood, 2015) and `stats` packages in R version V3.6.3 (R Core Team, 2020)
281 for our data analyses and `ggplot2` for visualisations (Wickham and Wickham, 2016). The significance
282 level for all tests was set at 0.05.

283 We used Kolmogorov-Smirnov tests (`ks.test` function) to evaluate the effects of contrasting seasons,
284 specifically the driest and wettest periods, on the distributions of CH_4 and N_2O fluxes at both ecosystem
285 and soil levels. A Student's t-test (`t.test` function) was used to determine if the greenhouse gas fluxes
286 were statistically different from 0. Generalised additive models (GAM; `gam` function) were used to
287 assess whether climate variables (i.e. R_g , T_s , SWC) explained the temporal variations in CH_4 and N_2O
288 fluxes at the ecosystem and soil levels. We included the default thin-plate spline smoothing parameter
289 selected by restricted maximum likelihood (REML), and modelled the fluxes of each greenhouse gas as



290 a function of season, climate variables and their interaction. For all GAMs, the “select” option was set
291 to TRUE so that terms could be removed from the GAM during model fitting if they provided no benefit
292 (Wood, 2017).

293

294 **3 Results**

295 **3.1 Environmental seasonality**

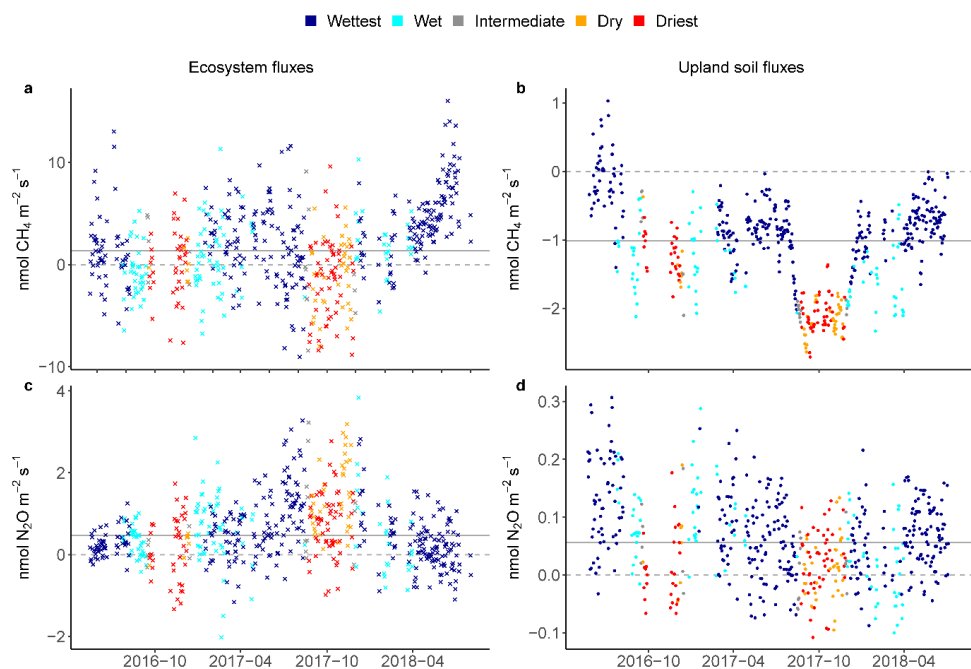
296 The Guyaflux site is characterised by an alternating wet and dry season, typical of a wet tropical
297 climate. During the wet season, mean daily global radiation (R_g ; Fig. 1a) was at its lowest, while soil
298 water content (SWC; Fig. 1b) was at its highest, accompanied by peak values for relative extractable
299 water (REW; Fig. 1c). In contrast, the dry season had elevated mean daily R_g , minimal SWC and the
300 lowest values of REW. The soil temperature (T_s ; Fig. 1d) also exhibited a clear seasonal pattern, albeit
301 weak in absolute values (approximately 2°C), which was influenced by changes in air temperature.
302 During the study period, the driest season (SWC ranging from 9.9% to 15.0%) covered 15.8% of the
303 total study period (128 days), while the wettest season (SWC ranging from 20.0% to 30.0%) covered
304 55% of the total study period (444 days) and represented near-saturated conditions.

305

306 **3.2 Greenhouse gas flux seasonality under contrasting environmental conditions**

307 The ecosystem and soil CH_4 and N_2O fluxes also displayed some seasonality (Figs. 2, S4, S5), with
308 seasonal differences particularly evident between the wettest and the driest season (Fig. 3).

309

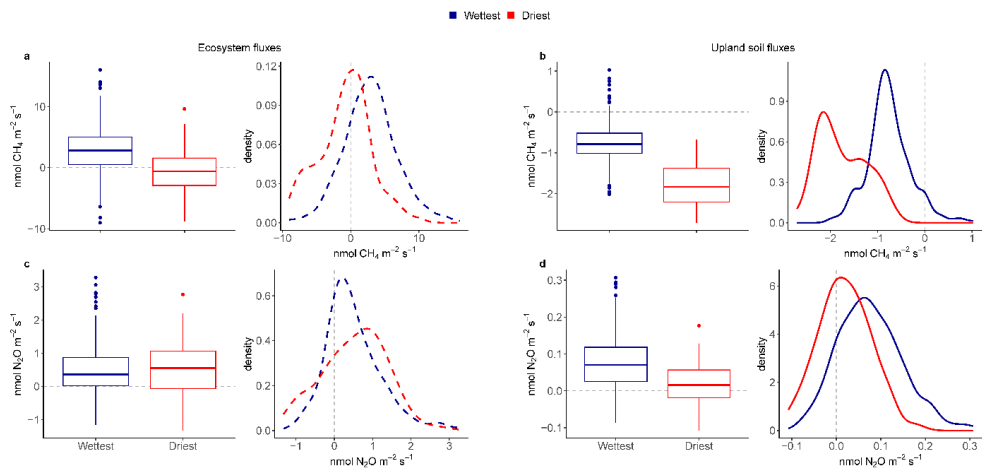


310

311 Figure 2. Seasonal courses of average daily ecosystem (crosses on the left) and upland soil (solid dots
312 on the right) fluxes for the wet, intermediate and dry seasons, and for two contrasted seasons defined
313 as the wettest (dark blue dots) and the driest (red dots) for 24-hour CH_4 fluxes (a, b) and N_2O fluxes
314 from 17 May, 2016 to 2 August, 2018 (c, d) in the Guyaflux tropical forest, French Guiana. Positive
315 fluxes (above the dashed grey “0” line) indicate greenhouse gas emissions and negative fluxes (below
316 the “0” line) indicate greenhouse gas uptake; the solid grey line represents the median over the whole
317 period. Note that the scale of the y-axis has been adjusted for each gas and compartment to improve
318 clarity.



319



320

321 Figure 3. Boxplots and associated density plots of average daily ecosystem fluxes (dashed lines on the
322 left) and upland soil (solid lines on the right) fluxes of 24-hour CH₄ fluxes (a, b) and N₂O fluxes (c, d) for
323 the wettest (blue) and driest (red) seasons, from 17 May, 2016 to 2 August, 2018 in the Guyaflux
324 tropical forest, French Guiana. In the box plots, solid bold lines represent medians, box boundaries
325 mark the 25th and 75th percentiles and whiskers show the 10th and 90th percentiles. Dots mark outliers.
326 In the density plots, positive fluxes on the right side of the dotted "0" line indicate greenhouse gas
327 emissions and negative fluxes on the left side of the "0" line indicate greenhouse gas uptake. All
328 differences among fluxes in the wettest and driest season were statistically significant at $p < 0.05$. See
329 Table 1 for the Kolmogorov-Smirnov test results.



CH₄ emissions were greater during the wettest season than during the driest season, when net fluxes hovered around zero (Table 1; Fig. 3a). In contrast to the ecosystem-level fluxes, soil CH₄ fluxes in some of the upland forest were mainly negative, indicating net soil CH₄ uptake throughout the year (Fig. 2b), even under varying environmental conditions (Table 1; Fig. 3b). Soil CH₄ uptake did decreased significantly in the wettest season compared to the driest season, although the fluxes remained negative overall (i.e. CH₄ uptake, Table 1; Fig. 3b).

336

Table 1. Mean, standard deviation (SD) and median ecosystem and upland soil CH₄ and N₂O fluxes for the wettest and driest seasons in the Guyaflux tropical forest, French Guiana. Values in bold are different from 0 at p level < 0.05 based on Student's t-test.

Fluxes	Wettest			Driest		
	Mean	SD	Median	Mean	SD	Median
Ecosystem flux (nmol_{CH4/N2O} m⁻² s⁻¹)						
CH₄	2.9	3.9	2.8	-0.8	3.8	-0.6
N₂O	0.5	0.7	0.4	0.5	0.8	0.6
Upland soil flux (nmol_{CH4/N2O} m⁻² s⁻¹)						
CH₄	-0.8	0.5	-0.8	-1.8	0.5	-1.8
N₂O	0.1	0.1	0.1	0.0	0.1	0.0

340

The seasonal pattern of ecosystem N₂O fluxes was less pronounced than for CH₄ (Fig. 2c); the driest season showed only slightly higher emissions than the wettest season (Table 1; Fig. 3c). In contrast to the ecosystem-level fluxes, soil N₂O fluxes in upland areas not only had a more pronounced seasonal pattern, the upland soils also emitted more N₂O during the wettest season than during the driest season, when the average flux was near-zero N₂O (Table 1; Fig. 3d). It is noteworthy that, although there were significant differences between seasons for all fluxes and at both ecosystem and soil levels (Fig. 3), the overall mean flux was significantly different from zero only for soil CH₄ fluxes during the driest season (Table 1). This indicates that the magnitude of the fluxes was very low relative to the large variability among the seasons.

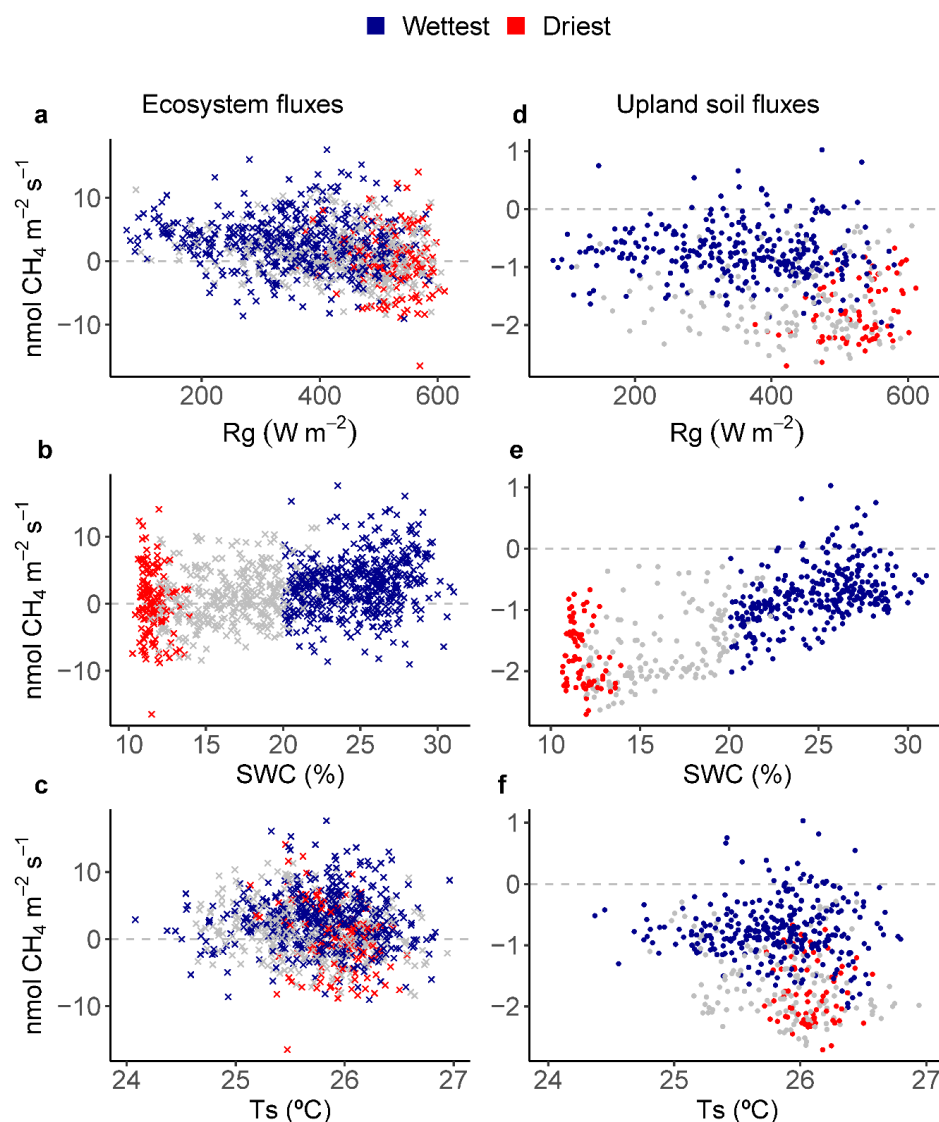


350

351 **3.3 Environmental drivers of ecosystem and upland soil greenhouse gas fluxes**

352 Net ecosystem CH₄ fluxes showed that CH₄ emissions decreased with increasing R_g (Fig. 4a), although
353 this negative correlation was statistically significant only during the wettest season (Table 2) when net
354 emissions occasionally switched to net uptakes at highest R_g values (Fig. 4a). Net ecosystem CH₄ fluxes
355 were strongly positively correlated with SWC (Fig. 4b), showing increased CH₄ emissions with
356 increasing SWC, although this correlation too was statistically significant only during the wettest
357 season (Table 2). A weaker, yet statistically significant, correlation was detected between ecosystem
358 CH₄ fluxes and T_s (Table 2).

359



360

361 Figure 4. Relationships between environmental drivers (global radiation (Rg), soil water content (SWC)
 362 and soil temperature (Ts)) and daily average ecosystem (crosses on the left) and upland soil (solid dots
 363 on the right) CH_4 fluxes for the wettest (blue) and driest (red) seasons, with remaining data in grey,
 364 from 17 May, 2016 to 2 August, 2018 in the Guyaflux tropical forest, French Guiana. Positive fluxes
 365 above the horizontal “0” line indicate CH_4 emissions and negative fluxes below the horizontal “0” line
 366 indicate CH_4 uptake.



367 Despite the different signs for the net CH₄ flux at ecosystem- and soil levels, relationships comparable
368 with the environmental drivers observed for ecosystem CH₄ fluxes were also found for some of the
369 upland soil: net soil CH₄ uptake increased with increasing R_g (Fig. 4d) and decreased with increasing
370 SWC (Fig. 4e). The correlation between upland soil CH₄ fluxes and R_g was statistically significant in the
371 driest season, while the correlation with SWC was equal and significant in both seasons (wettest and
372 driest, Table 2).

373 Ecosystem N₂O fluxes showed relatively weak responses to the environmental drivers we investigated
374 (Figs. 5a-c). The statistically significant terms in the model were SWC > R_g > T_s, and only during the
375 wettest season. However, the R² of the model was rather low (R² = 0.04; Table 2). For the upland soil
376 N₂O fluxes, none of the environmental drivers we investigated explained soil N₂O emissions (Fig. 5;
377 Table 2).

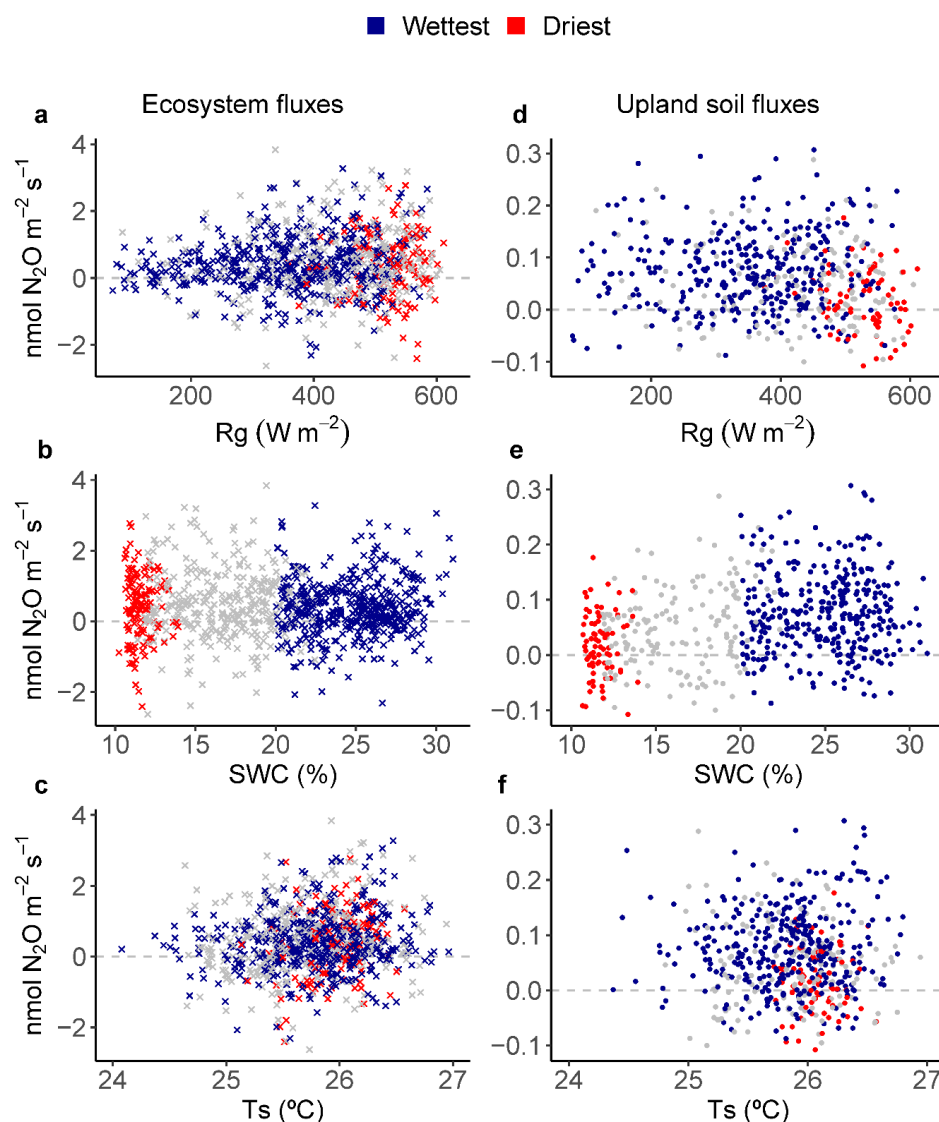
378



Table 2. Results of generalised additive models (GAM) assessing the relationships between environmental variables, i.e. global radiation (Rg), soil water content (SWC), soil temperature (Ts), and daily mean ecosystem and upland soil CH₄ and N₂O fluxes during the wettest and driest seasons from 17 May, 2016 to 2 August, 2018 in the Guyaflux tropical forest, French Guiana. The effective degrees of freedom (edf) and the reference number of degrees of freedom (Ref. df) of the fitted models, with values for each spline term, are shown. Significant terms at p level < 0.05 are shown in bold.

Fluxes	Best model predictors	R ²	Intercept	Coefficients		F value	p value	
				edf	Ref. df			
Ecosystem level								
Daily	CH ₄		0.20	0.002				
		Rg: Wettest			0.8	9	0.54	0.014
		Rg: Driest			0.6	8	0.19	0.113
		Ts: Wettest			1.7	9	0.62	0.025
		Ts: Driest			0.0	9	0.00	0.477
		SWC: Wettest			1.6	9	1.92	< 0.001
	SWC: Driest	0.0	6	0.00	0.433			
Daily	N ₂ O		0.04	0.000				
		Rg: Wettest			0.8	9	0.41	0.026
		Rg: Driest			0.0	8	0.00	0.772
		Ts: Wettest			1.2	9	0.39	0.045
		Ts: Driest			0.3	8	0.05	0.247
		SWC: Wettest			2.2	9	0.93	0.011
	SWC: Driest	0.0	6	0.00	0.717			
Upland soil level								
Daily	CH ₄		0.54	-0.001				
		Rg: Wettest			1.2	9	0.24	0.156
		Rg: Driest			1.5	9	1.24	0.001
		Ts: Wettest			0.7	9	0.27	0.057
		Ts: Driest			0.0	9	0.00	0.865
		SWC: Wettest			2.6	9	9.74	< 0.001
	SWC: Driest	1.9	7	3.52	< 0.001			
Daily	N ₂ O		0.10	0.000				
		Rg: Wettest			0.0	9	0.00	0.419
		Rg: Driest			0.6	8	0.19	0.112
		Ts: Wettest			1.2	9	0.32	0.084
		Ts: Driest			0.0	9	0.00	1.000
		SWC: Wettest			0.0	9	0.00	0.804
	SWC: Driest	0.0	6	0.00	1.000			

385



386

387 Figure 5. Relationships between environmental drivers (global radiation (R_g), soil water content (SWC)
388 and soil temperature (T_s)) and daily average ecosystem (crosses on the left) and upland soil (solid dots
389 on the right) N_2O fluxes for the wettest (blue) and driest (red) seasons, with remaining data in grey,
390 from 17 May, 2016 to 2 August, 2018 in the Guyaflux tropical forest, French Guiana. Positive fluxes
391 above the horizontal “0” line indicate N_2O emissions and negative fluxes below the horizontal “0” line
392 indicate N_2O uptake.



393

394 **4 Discussion**

395 To our knowledge, this is the first study to report on simultaneous ecosystem and upland soil CH₄ and
396 N₂O flux observations in a wet tropical forest over a period of more than two years (Fig. 2). This study
397 provides a unique opportunity to investigate the dynamics and environmental drivers of CH₄ and N₂O
398 fluxes in these ecosystems.

399

400 **4.1 Ecosystem and upland soil-CH₄ fluxes**

401 4.1.1 Seasonal variations in ecosystem CH₄ fluxes: trends and drivers

402 Our long-term monitoring of eddy covariance CH₄ fluxes above the Guyaflux forest canopy showed
403 high temporal variability, with changes in the sign (net emission or uptake) and amount of the
404 ecosystem fluxes observed over short time scales, supporting hypothesis H1 (Fig. 2). Net CH₄ emission
405 rates ($2.9 \pm 3.9 \text{ nmolCH}_4 \text{ m}^{-2} \text{ s}^{-1}$; Mean \pm SD) dominated during the wettest season, whereas net CH₄
406 uptake ($-0.8 \pm 3.8 \text{ nmolCH}_4 \text{ m}^{-2} \text{ s}^{-1}$) was more common during the driest season, although large
407 temporal variations occurred throughout the study seasons (Figs. 2-3, Table S1). Much higher wet-
408 season net fluxes had previously been found in two Brazilian tropical forests, Manaus and Sinop (62.3
409 and $34.6 \text{ nmolCH}_4 \text{ m}^{-2} \text{ s}^{-1}$, respectively; Carmo et al., 2006), though the studies were based on canopy
410 air samples and a modelling approach. Surprisingly, these Brazilian forests acted as an even larger CH₄
411 source during the driest season (64.1 and $88.3 \text{ nmolCH}_4 \text{ m}^{-2} \text{ s}^{-1}$, respectively; Carmo et al., 2006), while
412 the Guyaflux forest switched from a CH₄ source during the wet periods to a small sink during the dry
413 ones. Ecosystem CH₄ fluxes are driven by a combination of plant, microbial and abiotic processes,
414 which are mediated by both living and dead plants, and can explain episodic bursts (Eugster and Plüss,
415 2010; Covey and Megonigal, 2019). The mechanism underlying the large CH₄ emissions during the dry
416 season observed in the Brazilian forests remains unknown, but the authors suggest that it may have
417 been connected to the anaerobic decay of waterlogged wood, undrained soil patches or the
418 waterlogged cavities of tank bromeliads. Concomitantly, drought-induced reduced oxidation in the soil



419 surface layer may have exacerbated the net CH₄ emissions. Contrary to Carmo et al. (2006), Sakabe et
420 al. (2018) found a seasonal pattern similar to the one we observed in our study where the eddy
421 covariance technique was applied. Although the flux values they found had a higher range of variation
422 (10.3 nmolCH₄ m⁻² s⁻¹ versus -8.5 nmolCH₄ m⁻² s⁻¹, respectively, in the wet and dry seasons), this was
423 most likely due to the different ecosystem they studied, an Indonesian tropical peat swamp forest.
424 Consistent with H2, the generalised additive models (GAM) revealed that SWC, and to a lesser extent
425 Rg and Ts, were relevant ecosystem CH₄ flux drivers, particularly during the wettest season (Table 2;
426 Figs. 4a-c). It is reasonable to assume that high SWC but relatively low Ts during the wettest season
427 stimulated CH₄ production in most compartments of the ecosystem, not only in the seasonally flooded
428 soils. An increase in SWC at shallow depths may reduce the amount of air-filled pore space in the soil.
429 This reduction may decrease the diffusion of oxygen and CH₄ from the atmosphere through the soil to
430 methanotrophs, resulting in a decrease in net uptake or an increase in net emissions, if production
431 exceeds uptake (Wang et al., 2013). Such processes may occur in all the soil types within the footprint
432 of the eddy flux tower (see Sect. 4.1.2), and they may partially explain the seasonal trends observed at
433 our site. On the other hand, the statistically significant, albeit weak, relationship between CH₄
434 emissions and Rg during the wettest season could occur if the occasional high light intensity (Fig. 1a) is
435 sufficient to stimulate plant-mediated CH₄ transport through sap flow, and / or if the measured forest
436 area has more seasonally flooded areas than upland forest. The latter explanation is, however, unlikely
437 because the location of the Guyaflux tower (~300 m from the seasonally flooded area) was specifically
438 chosen to guarantee consistent types of ecosystem flux observations regardless of the season and of
439 associated changes in wind direction and atmospheric stability. Further research is needed to clarify
440 the correlation between Rg and net CH₄ flux. Increased fluxes in the flooded areas and anaerobic
441 microsites, rather than seasonal changes in the footprint, probably explain part of the observed
442 seasonal variations.

443 Disentangling the drivers of net CH₄ fluxes is further complicated by aboveground processes that also
444 contribute to CH₄ emissions and uptake in forest ecosystems. Soil-produced CH₄ dissolved in water can



indeed be taken up by roots, transported through the xylem stream in the stem, branches and leaves, and then released into the atmosphere, thus bypassing the oxidation processes in the shallow soil layers. As such, the highest CH₄ emissions from trees have been found in waterlogged soils, for example, in wetland and riparian forests (Pangala et al., 2013; Covey and Megonigal, 2019; Gauci et al., 2025). However, recent studies have shown that tree compartments (i.e. stems, branches, and leaves) can also consume CH₄, particularly in free-draining upland soils (Gauci et al., 2024). At our study site, both stem CH₄ emission and uptake were observed within the footprint of the Guyaflux tower (Bréchet et al., 2021, 2025; Daniel et al., 2023). Although these fluxes were weak, they contributed to the seasonal variations in ecosystem CH₄ exchanges (Bréchet et al., 2021, 2025; Daniel et al., 2023).

4.1.2 Seasonal variations in upland soil CH₄ fluxes: trends and drivers

The upland soils studied within the tower footprint were active consumers of atmospheric CH₄ (Fig. 3b), with overall net uptake rates of $1.1 \pm 0.7 \text{ nmolCH}_4 \text{ m}^{-2} \text{ s}^{-1}$, which is higher than the global average for tropical forests ($-0.7 \text{ nmolCH}_4 \text{ m}^{-2} \text{ s}^{-1}$ or $-2.5 \text{ kgCH}_4\text{-C ha}^{-1} \text{ yr}^{-1}$, Dutaur and Verchot, 2007) but lower than fluxes found in previous studies in tropical plantations and forests in Central and South America (Panama, $-13.5 \text{ nmolCH}_4 \text{ m}^{-2} \text{ s}^{-1}$, Keller et al., 1990; $-19.9 \text{ nmolCH}_4 \text{ m}^{-2} \text{ s}^{-1}$, Goreau and de Mello, 1988). CH₄ fluxes at our site ranged seasonally from $-0.8 \pm 0.5 \text{ nmolCH}_4 \text{ m}^{-2} \text{ s}^{-1}$ in the wettest season to $-1.8 \pm 0.5 \text{ nmolCH}_4 \text{ m}^{-2} \text{ s}^{-1}$ in the driest season (Table S2), supporting H1 and globally corroborating other seasonal studies in tropical forests. In addition, CH₄ flux dynamics in our upland soils were characterised by a large range of variation, but a consistent sign, between the driest and wettest seasons. A study conducted in a seasonal tropical forest in China with static chambers showed a comparable seasonal pattern for soils: they acted mainly as CH₄ consumers, with an uptake rate of $0.7 \pm 0.0 \text{ nmolCH}_4 \text{ m}^{-2} \text{ s}^{-1}$ (or $29.5 \pm 0.3 \text{ } \mu\text{gCH}_4\text{-C m}^{-2} \text{ h}^{-1}$; Werner et al., 2006) during the dry period. The uptake decreased by approximately 50% after the first rainfall events and the associated increases in SWC. Another study carried out with the static chamber technique near the Guyaflux forest and in similar environmental conditions reported that upland soils consumed $1.0 \pm 3.2 \text{ nmolCH}_4 \text{ m}^{-2} \text{ s}^{-1}$ during



471 the dry season (Courtois et al., 2018). Yet, those soils become slight emitters during the wet season
472 ($0.1 \pm 0.9 \text{ nmolCH}_4 \text{ m}^{-2} \text{ s}^{-1}$; corresponding to $-44.0 \pm 139.7 \text{ } \mu\text{gCH}_4\text{-C m}^{-2} \text{ h}^{-1}$ and $3.7 \pm 40.1 \text{ } \mu\text{gCH}_4\text{-C m}^{-2}$
473 h^{-1} for the dry and wet seasons, respectively; Courtois et al., 2018). However, although meaningful,
474 these comparisons between studies should be interpreted with great caution because the
475 measurement techniques differed (i.e. automated in our study versus manual chambers in the other
476 studies).

477 The best set of meteorological parameters, explaining 53% of the seasonal variation in CH_4 fluxes from
478 upland soils, were SWC, T_s and R_g (Table 2), consistent with H2. We observed a net upland soil CH_4
479 uptake during both the driest and the wettest seasons; CH_4 emissions occurred only on a few days
480 during the wettest season (Fig. 2b). This can likely be explained by the soil characteristics at our site
481 where upland soils were hypoferralic Acrisols, characterised by deep vertical drainage (Epron et al.,
482 2006). It is likely that these well aerated soils provided the aerobic conditions for methanotrophic CH_4
483 oxidation (Smith et al., 2003). The seasonal variations in net CH_4 fluxes were strong (Fig. 3b) with a net
484 soil CH_4 uptake twice as high in the driest season as in the wettest season. This is consistent with the
485 known dependence of soil CH_4 fluxes on topsoil SWC (Fig. 4e; Tables 1, 3): dryer soil conditions favour
486 soil methanotrophy (Le Mer and Roger, 2001) and wet soils reduce methanotrophic communities and
487 / or their activity (Covey and Megonigal, 2019).

488

489 **4.2 Ecosystem and upland soil- N_2O fluxes**

490 **4.2.1 Seasonal variations in ecosystem N_2O fluxes: trends and drivers**

491 The measurements at the Guyaflux wet-tropical-forest site revealed very low N_2O fluxes, with an
492 average net emission of $0.6 \pm 0.8 \text{ nmolN}_2\text{O m}^{-2} \text{ s}^{-1}$ (Fig. 3c; Table 1). Though low, this loss of nitrogen
493 (N) from the ecosystem is equivalent to approximately one-fifth of the annual atmospheric N
494 deposition at the site ($2.7 \text{ kgN}_2\text{O-N ha}^{-1} \text{ yr}^{-1}$ here vs. $13 \text{ kgN}_2\text{O-N ha}^{-1} \text{ yr}^{-1}$ in Van Langenhove et al.,
495 2020). Compared to other publications on forest ecosystem N_2O fluxes from studies based on eddy
496 covariance techniques, net ecosystem N_2O fluxes at our study site were very close to the average fluxes



497 reported by Stiegler et al. (2023) for a regularly-fertilised Indonesian oil palm plantation (0.7 ± 0.0
498 $\text{nmolN}_2\text{O m}^{-2} \text{s}^{-1}$ or $0.32 \pm 0.003 \text{ gN}_2\text{O-N m}^{-2} \text{yr}^{-1}$) but much higher than those reported by Mander et al.
499 (2021) for a temperate riparian deciduous forest ($0.1 \text{ nmolN}_2\text{O m}^{-2} \text{s}^{-1}$ or $87.3 \text{ mgN}_2\text{O-N m}^{-2}$ for the
500 September 2017 - December 2019 period).

501 Measured ecosystem-level N_2O fluxes at the Guyaflux site were highly variable, but overall showed
502 little seasonal variation (means of $0.5 \pm 0.8 \text{ nmolN}_2\text{O m}^{-2} \text{s}^{-1}$ and $0.5 \pm 0.7 \text{ nmolN}_2\text{O m}^{-2} \text{s}^{-1}$, in the driest
503 and the wettest seasons, respectively; Table S2), partially supporting H1. These observations fall within
504 the range of net ecosystem N_2O exchanges measured by eddy covariance reported in an oil palm
505 plantation in Indonesia, with similar mean N_2O emissions of $0.7 \text{ nmolN}_2\text{O m}^{-2} \text{s}^{-1}$ for both the dry and
506 wet seasons (Stiegler et al., 2023). Once again, this comparison must be interpreted with extreme
507 caution even though both studies used the eddy covariance technique as the ecosystems and seasons
508 concerned were different (a tropical oil palm plantation with strong seasons versus a primary wet
509 tropical forest).

510 As with CH_4 fluxes, the temporal variability of the N_2O fluxes was very high (Fig. 2c). Contrary to H2,
511 GAM analyses failed to explain or attribute the observed variations in N_2O fluxes to changes in SWC or
512 other meteorological drivers ($R^2 = 0.04$, Table 2). Furthermore, daily mean ecosystem N_2O fluxes
513 switched signs and changed in order of magnitude on short time scales, most likely because these
514 fluxes are controlled by discontinuous microbial processes (Blagodatsky and Smith, 2012). Yet, we did
515 find statistically significant, though very weak, relationships between ecosystem N_2O fluxes and SWC,
516 T_s and R_g , suggesting that the wettest season may provide favourable conditions for soil bacterial N_2O
517 production and plant-mediated N_2O transport, which could contribute to higher net N_2O emissions at
518 the ecosystem level (Stiegler et al., 2023). It is worth noting that the extent to which trees mediate N_2O
519 emissions is still uncertain; at Guyaflux, within the tower footprint, tree stems in the seasonally flooded
520 forest emit N_2O while those in the upland forest absorb N_2O (Daniel et al., 2023). Other studies at
521 Guyaflux and in a lowland tropical rain forest in the Réunion Islands reported that tree stems can
522 absorb N_2O through as yet unknown mechanisms (Bréchet et al., 2021, 2025; Machacova et al., 2021).



523 This could indeed counteract the overriding, albeit small, net ecosystem N₂O emissions, suggesting
524 that the proportion of upland versus seasonal areas should be taken into account.

525

526 4.2.2 Seasonal variations in upland soil N₂O fluxes: trends and drivers

527 In support of H1, N₂O fluxes recorded for the upland soils studied were small, averaging 0.1 ± 0.1
528 $\text{nmolN}_2\text{O m}^{-2} \text{s}^{-1}$ (Table 1, S2), and slightly higher during the wettest season ($0.1 \pm 0.1 \text{ nmolN}_2\text{O m}^{-2} \text{s}^{-1}$)
529 compared to the driest season ($0.0 \pm 0.1 \text{ nmolN}_2\text{O m}^{-2} \text{s}^{-1}$; Table S2). Our flux values were nine times
530 smaller than those measured with automated chamber systems in a western Kenyan rainforest (0.9
531 $\text{nmolN}_2\text{O m}^{-2} \text{s}^{-1}$; Werner et al., 2007), even though the soils in both cases were predominantly N₂O
532 emitters. However, our seasonal N₂O flux observations were within the same order of magnitude as
533 those in two tropical rainforests where soil N₂O emissions measured with manual chambers were
534 lower in the dry season than in the wet season ($< 0.20 \text{ nmolN}_2\text{O m}^{-2} \text{s}^{-1}$ and $0.34 \text{ nmolN}_2\text{O m}^{-2} \text{s}^{-1}$,
535 respectively, in Yu et al., 2021; $0.10 \text{ nmolN}_2\text{O m}^{-2} \text{s}^{-1}$ and $0.49 \text{ nmolN}_2\text{O m}^{-2} \text{s}^{-1}$, respectively, in Werner
536 et al., 2006).

537 In contrast to H2, none of our GAMs including meteorological drivers (i.e. SWC, Ts, Rg) predicted the
538 observed seasonal variations in upland soil N₂O fluxes when only the driest and wettest seasons were
539 taken into account (Table 2; Fig. 5). However, when all the seasons were accounted for, an increase in
540 SWC appeared to partially explain the increase in soil N₂O fluxes (Figs. 5e, S5d). Although both
541 nitrification and denitrification can occur simultaneously in various soil microsites (Stevens et al.,
542 1997), N₂O release often occurs on a daily basis in environments with rapidly shifting O₂ availability,
543 which is the case for soils with changing SWC (Davidson, 1992; Fig. 1). Several studies in subtropical
544 and tropical forests have reported significant effects of SWC on tropical soil N₂O fluxes (Kiese and
545 Butterbach-Bahl, 2002; Werner et al., 2006, 2007; Gütlein et al., 2018).

546



547 **5 Conclusion**

548 Our long-term monitoring of ecosystem and soil CH₄ and N₂O fluxes over a period of 26 months under
549 contrasting climatic conditions (driest versus wettest seasons) revealed highly variable fluxes that
550 changed direction and amount on short time scales. Although mean daily fluxes were low, N₂O
551 emissions were observed all year long. In contrast, for CH₄, either emission or uptake occurred,
552 depending on the season. As expected, the seasons had a statistically significant effect on ecosystem
553 CH₄ and N₂O fluxes, with CH₄ uptake and higher N₂O emissions during the driest season than during
554 the wettest season. Upland soils exhibited highly variable CH₄ and N₂O fluxes, with an increase in CH₄
555 uptake and a decrease in N₂O emissions from the wettest to the driest season. The climatic variables
556 we selected explained only a minor part of the seasonal variations in ecosystem CH₄ and N₂O fluxes.
557 At the soil level, none of the climatic variables were significant for seasonal fluxes of N₂O whereas SWC
558 was a strong driver of CH₄ fluxes.

559 Measurements at the ecosystem and soil levels showed divergent fluxes, probably because soil fluxes
560 represent only one compartment in the whole ecosystem. Furthermore, upland soils (52% of the
561 footprint area) are only one type of soil within the large range of soils found inside the Guyaflux tower
562 footprint. In addition, soil chambers provide integrated fluxes for a much smaller area than does the
563 eddy covariance technique. In order to improve the understanding of seasonal variations in ecosystem
564 CH₄ and N₂O fluxes, our study shows that it is crucial to characterise the fluxes for all existing ecosystem
565 compartments at the same time and to include all the tree components (leaves, stems, branches) and
566 tree species in the forest habitats, not just those on upland soils. However, our study still provides
567 valuable data that, when combined with mechanistic models, may help identify the missing drivers
568 responsible for the seasonal variations in CH₄ and N₂O fluxes in wet tropical forest ecosystems.

569



570 **Data availability**

571 All raw data can be provided by the corresponding authors upon request.

572

573 **Supplement link**

574

575 **Author contributions**

576 LMB, MI, CS, DB, IAJ conceived the ideas and designed the methodology; LMB and BB collected the
577 data; LMB and MI performed quality control checks on the data and analysed the data; IAJ and RBJ
578 obtained the funding; LMB led the writing of the manuscript and all authors contributed to the
579 manuscript and gave final approval for submission.

580

581 **Competing interests**

582 The authors declare that they have no conflict of interest.

583

584 **Acknowledgements**

585 We would like to thank Jean-Yves Goret, Nicola Arriga and Elodie Courtois for their technical support.

586 We thank Vicki Moore for correcting the English of this paper.

587

588 **Financial support**

589 This work was supported by the European Research Council Synergy grant ERC-2013-SyG-610028-
590 IMBALANCE-P and the European Commission through a Marie Skłodowska-Curie Individual Fellowship
591 H2020-MSCA-IF-2017-796438 awarded to L. M. Bréchet, the UMR “Ecologie des Forêts de Guyane”
592 (EcoFoG) and the Research Fund of the University of Antwerp. This work was also supported by the
593 Gordon and Betty Moore Foundation, Stanford University and the National Research Institute for
594 Agriculture, Food and Environment (INRAE) through the Gordon and Betty Moore Foundation grant



595 GBMF-11519 for L. M. Bréchet's Postdoctoral Fellowship, and by an Investissement d'Avenir grant from
596 the Agence Nationale de la Recherche (CEBA: ANR-10-LABX-25-01).

597

598 **References**

599 Aguilos, M., Hérault, B., Burban, B., Wagner, F., Bonal, D.: What drives long-term variations in carbon
600 flux and balance in a tropical rainforest in French Guiana?, *Agric. For. Meteorol.*, 253–254, 114–
601 123, <https://doi.org/10.1016/j.agrformet.2018.02.009>, 2018.

602 Aubinet, M., Grelle, A., Ibrom, A., Rannik, Ü., Moncrieff, J., Foken, T., Kowalski, A. S., Martin, P. H.,
603 Berbigier, P., Bernhofer, C., Clement, R., Elbers, J., Granier, A., Grünwald, T., Morgenstern, K.,
604 Pilegaard, K., Rebmann, C., Snijders, W., Valentini, R., Vesala, T.: Estimates of the annual net
605 carbon and water exchange of European forests: the EUROFLUX methodology, *Adv. Ecol. Res.*,
606 30, 114–175, [https://doi.org/10.1016/S0065-2504\(08\)60018-5](https://doi.org/10.1016/S0065-2504(08)60018-5), 2000.

607 Aubinet, M., Vesala, T. and Papale, D. eds.: Eddy covariance: a practical guide to measurement and
608 data analysis, Springer Science and Business Media, 2012.

609 Baldocchi, D. D.: Assessing the eddy covariance technique for evaluating carbon dioxide exchange rates
610 of ecosystems: past, present and future, *Glob. Chang. Biol.*, 9, 479–92,
611 <https://doi.org/10.1046/j.1365-2486.2003.00629.x>, 2003.

612 Baldocchi, D.: Measuring fluxes of trace gases and energy between ecosystems and the atmosphere -
613 the state and future of the eddy covariance method, *Glob. Chang. Biol.*, 20, 3600–9,
614 <https://doi.org/10.1111/gcb.12649>, 2014.

615 Baldocchi, D. D.: How eddy covariance flux measurements have contributed to our understanding of
616 Global Change Biology, *Glob. Chang. Biol.*, 26, 242–60, <https://doi.org/10.1111/gcb.14807>, 2020.

617 Bernhardt, E. S., Blaszcak, J. R., Ficken, C. D., Fork, M. L., Kaiser, K. E., Seybold, E. C.: Control points in
618 ecosystems: moving beyond the hot spot hot moment concept, *Ecosystems*, 20, 665–82,
619 <https://doi.org/10.1007/s10021-016-0103-y>, 2017.

620 Blagodatsky, S., Smith P.: Soil physics meets soil biology: towards better mechanistic prediction of



621 greenhouse gas emissions from soil, *Soil Biol. Biochem.*, 47, 78–92,
622 <https://doi.org/10.1016/j.soilbio.2011.12.015>, 2012.

623 Bonal, D., Bosc, A., Ponton, S., Goret, J.-Y., Burban, B. T., Gross, P., Bonnefond, J. M., Elbers, J., Longdoz,
624 B., Epron, D., Guehl, J. M., Granier, A.: Impact of severe dry season on net ecosystem exchange
625 in the Neotropical rainforest of French Guiana, *Glob. Chang. Biol.*, 14, 1917–1933,
626 <https://doi.org/10.1111/j.1365-2486.2008.01610.x>, 2008.

627 Bouwman, A. F., Fung, I., Matthews, E., John, J.: Global analysis of the potential for N₂O production in
628 natural soils, *Global Biogeochem. Cy.*, 7, 557–597, <https://doi.org/10.1029/93GB01186>, 1993.

629 Bréchet, L. M., Daniel, W., Stahl, C., Burban, B., Goret, J.-Y., Salomón, R. L., Janssens, I. A.: Simultaneous
630 tree stem and soil greenhouse gas (CO₂, CH₄, N₂O) flux measurements: a novel design for
631 continuous monitoring towards improving flux estimates and temporal resolution, *New Phytol.*,
632 230, 2487–500, <https://doi.org/10.1111/nph.17352>, 2021.

633 Bréchet, L. M., Salomón, R. L., Machacova, K., Stahl, C., Burban, B., Goret, J.-Y., Steppe, K., Bonal, D.,
634 Janssens, I. A.: Insights into the subdaily variations in methane, nitrous oxide and carbon dioxide
635 fluxes from upland tropical tree stems, *New Phytol.*, 245, 2451–2466,
636 <https://doi.org/10.1111/nph.20401>, 2025.

637 Carmo, J. B., Keller, M., Dias, J. D., Camargo, P. B., Crill, P.: A source of methane from upland forests in
638 the Brazilian Amazon, *Geophys. Res. Lett.*, 33, 4, <https://doi.org/10.1029/2005GL025436>, 2006.

639 Courtois, E. A., Stahl, C., Van den Berge, J., Bréchet, L., Van Langenhove, L., Richter, A., Urbina, I., Soong,
640 J. L., Penuelas, J., Janssens, I. A.: Spatial variation of soil CO₂, CH₄ and N₂O fluxes across
641 topographical positions in tropical forests of the guiana shield, *Ecosystems*, 21, 1445–58,
642 <https://doi.org/10.1007/s10021-018-0232-6>, 2018.

643 Courtois, E. A., Stahl, C., Burban, B., Van den Berge, J., Berveiller, D., Bréchet, L., Soong, J. L., Arriga, N.,
644 Peñuelas, J., Janssens, I. A.: Automatic high-frequency measurements of full soil greenhouse gas
645 fluxes in a tropical forest, *Biogeosciences*, 16, 785–96, <https://doi.org/10.5194/bg-16-785-2019>,
646 2019.



- 647 Covey, K. R., Megonigal, J. P.: Methane production and emissions in trees and forests, *New Phytol.*,
648 222, 35–51, <https://doi.org/10.1111/nph.15624>, 2019.
- 649 Covey, K., Soper, F., Pangala, S., Bernardino, A., Pagliaro, Z., Basso, L., Cassol, H., Fearnside, P.,
650 Navarrete, D., Novoa, S., Sawakuchi, H.: Carbon and beyond: The biogeochemistry of climate in a
651 rapidly changing Amazon, *Front. For. Glob. Change.*, 4, 1–20,
652 <https://doi.org/10.3389/ffgc.2021.618401>, 2021.
- 653 Daniel, W., Stahl, C., Burban, B., Goret, J.-Y., Cazal, J., Richter, A., Janssens, I. A., Bréchet, L. M.: Tree
654 stem and soil methane and nitrous oxide fluxes, but not carbon dioxide fluxes, switch sign along
655 a topographic gradient in a tropical forest, *Plant Soil*, 488, 533–49,
656 <https://doi.org/10.1007/s11104-023-05991-y>, 2023.
- 657 Davidson, E.A.: Sources of nitric oxide and nitrous oxide following wetting of dry soil, *Soil Sci. Soc. Am.*
658 J., 56, 95–102, <https://doi.org/10.2136/sssaj1992.03615995005600010015x>, 1992.
- 659 Davidson, E. A., De Araújo, A. C., Artaxo, P., Balch, J. K., Brown, I. F., Mercedes, M. M., Coe, M. T.,
660 Defries, R. S., Keller, M., Longo, M., Munger, J. W., Schroeder, W., Soares-Filho, B. S., Souza, C.
661 M., Wofsy, S. C., The Amazon basin in transition, *Nature*, 481, 321–328,
662 <https://doi.org/10.1038/nature10717>, 2012.
- 663 Delwiche, K. B., Knox, S. H., Malhotra, A., Fluet-Chouinard, E., McNicol, G., Feron, S., Ouyang, Z., Papale,
664 D., Trotta, C., Canfora, E., Cheah, Y. W.: FLUXNET-CH₄: A global, multi-ecosystem dataset and
665 analysis of methane seasonality from freshwater wetlands, *Earth Syst. Sci. Data Discuss.*, 2021,
666 1–11, <https://doi.org/10.5194/essd-13-3607-2021>, 2021.
- 667 Dutaur, L., Verchot, L.V.: A global inventory of the soil CH₄ sink. *Global Biogeochem. Cy.*, 21, 4,
668 <https://doi.org/10.1029/2006GB002734>, 2007.
- 669 Epron, D., Bosc, A., Bonal, D., Freycon, V.: Spatial variation of soil respiration across a topographic
670 gradient in a tropical rain forest in French Guiana, *J. Trop. Ecol.*, 22, 565–74,
671 <https://doi.org/10.1017/S0266467406003415>, 2006.
- 672 Eugster, W., Plüss, P.: A fault-tolerant eddy covariance system for measuring CH₄ fluxes, *Agric. For.*



- 673 Meteorol., 150, 841–51, <https://doi.org/10.1016/j.agrformet.2009.12.008>, 2010.
- 674 Eugster, W., Merbold, L.: Eddy covariance for quantifying trace gas fluxes from soils, *Soil*, 1, 187–205,
675 <https://doi.org/10.5194/soil-1-187-2015>, 2015.
- 676 Fang, J., Fang, J., Chen, B., Zhang, H., Dilawar, A., Guo, M. and Liu, S.A.: Assessing spatial
677 representativeness of global flux tower eddy-covariance measurements using data from
678 FLUXNET2015, *Sci. Data*, 11, 569, <https://doi.org/10.1038/s41597-024-03291-3>, 2024.
- 679 von Fischer, J. C., Hedin, L. O.: Controls on soil methane fluxes: Tests of biophysical mechanisms using
680 stable isotope tracers, *Global Biogeochem. Cy.*, 21, 9-Gb2007,
681 <https://doi.org/10.1029/2006gb002687>, 2007.
- 682 Gauci, V.: Tree methane exchange in a changing world, *Nat. Rev. Earth Environ.*, 6, 471–483,
683 <https://doi.org/10.1038/s43017-025-00692-9>, 2025.
- 684 Gauci, V., Pangala, S. R., Shenkin, A., Barba, J., Bastviken, D., Figueiredo, V., Gomez, C., Enrich-Prast, A.,
685 Sayer, E., Stauffer, T., Welch, B.: Global atmospheric methane uptake by upland tree woody
686 surfaces, *Nature*, 631, 796–800, <https://doi.org/10.1038/s41586-024-07592-w>, 2024.
- 687 Goreau, T. J., De Mello, W. Z.: Tropical deforestation: some effects on atmospheric chemistry, *Ambio.*,
688 17, 275–281, 1988.
- 689 Groffman, P. M., Butterbach-Bahl, K., Fulweiler, R. W., Gold, A. J., Morse, J. L., Stander, E. K., Tague, C.,
690 Tonitto, C., Vidon, P.: Challenges to incorporating spatially and temporally explicit phenomena
691 (hotspots and hot moments) in denitrification models, *Biogeochemistry*, 93, 49–77,
692 <https://doi.org/10.1007/s10533-008-9277-5>, 2009.
- 693 Gütlein, A., Gerschlauer, F., Kikoti, I., Kiese, R.: Impacts of climate and land use on N₂O and CH₄ fluxes
694 from tropical ecosystems in the Mt. Kilimanjaro region, Tanzania, *Glob. Chang. Biol.*, 24, 1239–
695 55, <https://doi.org/10.1111/gcb.13944>, 2018.
- 696 Ito, A., Inatomi, M.: Use of a process-based model for assessing the methane budgets of global
697 terrestrial ecosystems and evaluation of uncertainty, *Biogeosciences*, 9, 759–73,
698 <https://doi.org/10.5194/bg-9-759-2012>, 2012.



- 699 IUSS Working Group WRB: World reference base for soil resources 2014, update 2015. International
700 soil classification system for naming soils and creating legends for soil maps, World Soil Resources
701 Reports No. 106. FAO, Rome (2015), 2015.
- 702 Jones, C. M., Spor, A., Brennan, F. P., Breuil, M. C., Bru, D., Lemanceau, P., Griffiths, B., Hallin, S.,
703 Philippot, L.: Recently identified microbial guild mediates soil N₂O sink capacity, *Nat. Clim.*
704 *Change*, 4, 801–5, <https://doi.org/10.1038/nclimate2301>, 2014.
- 705 Keller, M., Mitre, M. E., Stallard, R. F.: Consumption of atmospheric methane in soils of central Panama:
706 effects of agricultural development, *Global Biogeochem. Cy.*, 4, 21–27,
707 <https://doi.org/10.1029/GB004i001p00021>, 1990.
- 708 Khalil, K., Mary, B., Renault, P.: Nitrous oxide production by nitrification and denitrification in soil
709 aggregates as affected by O₂ concentration, *Soil Biol. Biochem.*, 36, 687–99,
710 <https://doi.org/10.1016/j.soilbio.2004.01.004>, 2004.
- 711 Kiese, R., Butterbach-Bahl, K.: N₂O and CO₂ emissions from three different tropical forest sites in the
712 wet tropics of Queensland, Australia, *Soil Biol. Biochem.*, 34, 975–87,
713 [https://doi.org/10.1016/S0038-0717\(02\)00031-7](https://doi.org/10.1016/S0038-0717(02)00031-7), 2002.
- 714 Knox, S. H., Bansal, S., McNicol, G., Schafer, K., Sturtevant, C., Ueyama, M., Valach, A. C., Baldocchi, D.,
715 Delwiche, K., Desai, A. R., Euskirchen, E., et al.: Identifying dominant environmental predictors of
716 freshwater wetland methane fluxes across diurnal to seasonal time scales, *Glob. Chang. Biol.*, 27,
717 3582–604, <https://doi.org/10.1111/gcb.15661>, 2021.
- 718 Le Mer, J., Roger, P.: Production, oxidation, emission and consumption of methane by soils: a review,
719 *Eur. J. Soil Biol.*, 37, 25–50, [https://doi.org/10.1016/S1164-5563\(01\)01067-6](https://doi.org/10.1016/S1164-5563(01)01067-6), 2001.
- 720 Liu, Z., Li, H., Wu, F., Wang, H., Chen, H., Zhu, Q., Yang, G., Liu, W., Chen, D., Li, Y., Peng, C.:
721 Quantification of ecosystem-scale methane sinks observed in a tropical rainforest in Hainan,
722 China, *Land*, 11, 154, <https://doi.org/10.3390/land11020154>, 2022.
- 723 Lucas-Moffat, A. M., Huth, V., Augustin, J., Brummer, C., Herbst, M., Kutsch, W. L.: Towards pairing plot
724 and field scale measurements in managed ecosystems: Using eddy covariance to cross-validate



- 725 CO₂ fluxes modeled from manual chamber campaigns, *Agric. For. Meteorol.*, 256, 362–378,
726 <https://doi.org/10.1016/j.agrformet.2018.01.023>, 2018.
- 727 Machacova, K., Bäck, J., Vanhatalo, A., Halmeenmäki, E., Kolari, P., Mammarella, I., Pumpanen, J.,
728 Acosta, M., Urban, O., Pihlatie, M.: *Pinus sylvestris* as a missing source of nitrous oxide and
729 methane in boreal forest, *Sci. Rep.*, 6, 23410, <https://doi.org/10.1038/s41598-017-13781-7>,
730 2016.
- 731 Machacova, K., Borak, L., Agyei, T., Schindler, T., Soosaar, K., Mander, Ü., Ah-Peng, C.: Trees as net sinks
732 for methane (CH₄) and nitrous oxide (N₂O) in the lowland tropical rain forest on volcanic Réunion
733 Island, *New Phytol.*, 229, 1983–94, <https://doi.org/10.1111/nph.17002>, 2021.
- 734 Mander, Ü., Krasnova, A., Escuer-Gatius, J., Espenberg, M., Schindler, T., Machacova, K., Pärn, J.,
735 Maddison, M., Megonigal, J. P., Pihlatie, M., Kasak, K.: Forest canopy mitigates soil N₂O emission
736 during hot moments, *npj Clim. Atmos. Sci.*, 4, 39, <https://doi.org/10.1038/s41612-021-00194-7>,
737 2021.
- 738 Mauder, M., Foken, T.: Documentation and instruction manual of the eddy covariance software
739 package TK2, Universität Bayreuth, Abt. Mikrometeorologie, Arbeitsergebnisse 26:44 pp.
740 Internet, ISSN 1614–8926, 2004.
- 741 Nickerson, N.: Evaluating gas emission measurements using Minimum Detectable Flux (MDF), Eosense
742 Inc., Dartmouth, Nova Scotia, Canada, 2016.
- 743 Nicolini, G., Aubinet, M., Feigenwinter, C., Heinesch, B., Lindroth, A., Mamadou, O., Moderow, U.,
744 Mölder, M., Montagnani, L., Rebmann, C., Papale, D., Impact of CO₂ storage flux sampling
745 uncertainty on net ecosystem exchange measured by eddy covariance, *Agric. For. Meteorol.*, 248,
746 228–239, <https://doi.org/10.1016/j.agrformet.2017.09.025>, 2018.
- 747 Oertel, C., Matschullat, J., Zurba, K., Zimmermann, F., Erasmi, S.: Greenhouse gas emissions from
748 soils—A review, *Geochem.*, 76, 327–52, <https://doi.org/10.1016/j.chemer.2016.04.002>, 2016.
- 749 Pangala, S. R., Moore, S., Hornibrook, E. R., Gauci, V.: Trees are major conduits for methane egress
750 from tropical forested wetlands, *New Phytol.*, 197, 524–31, <https://doi.org/10.1111/nph.12031>,



- 751 2013.
- 752 Pitz, S., Megonigal, J. P.: Temperate forest methane sink diminished by tree emissions, *New Phytol.*,
753 214, 1432–9, <https://doi.org/10.1111/nph.14559>, 2017.
- 754 Sakabe, A., Itoh, M., Hirano, T., Kusin, K.: Ecosystem-scale methane flux in tropical peat swamp forest
755 in Indonesia, *Glob. Chang. Biol.*, 24, 5123–36, <https://doi.org/10.1111/gcb.14410>, 2018.
- 756 Sanford, R. A., Wagner, D. D., Wu, Q., Chee-Sanford, J. C., Thomas, S. H., Cruz-García, C., Rodríguez, G.,
757 Massol-Deyá, A., Krishnani, K. K., Ritalahti, K. M., Nissen, S.: Unexpected nondenitrifier nitrous
758 oxide reductase gene diversity and abundance in soils, *Proc. Natl. Acad. Sci.*, 109, 19709–14,
759 <https://doi.org/10.1073/pnas.1211238109>, 2012.
- 760 Silver, W. L., Lugo, A., Keller, M.: Soil oxygen availability and biogeochemistry along rainfall and
761 topographic gradients in upland wet tropical forest soils, *Biogeochemistry*, 44, 301–328,
762 <https://doi.org/10.1007/BF00996995>, 1999.
- 763 Smith, K. A., Ball, T., Conen, F., Dobbie, K. E., Massheder, J., Rey, A.: Exchange of greenhouse gases
764 between soil and atmosphere: interactions of soil physical factors and biological processes, *Eur.*
765 *J. soil sci.*, 54, 779–91, <https://doi.org/10.1046/j.1351-0754.2003.0567.x>, 2003.
- 766 Stevens, R. J., Laughlin, R. J., Burns, L. C., Arah, J. R., Hood, R. C.: Measuring the contributions of
767 nitrification and denitrification to the flux of nitrous oxide from soil, *Soil Biol. Biochem.*, 29, 139–
768 51, [https://doi.org/10.1016/S0038-0717\(96\)00303-3](https://doi.org/10.1016/S0038-0717(96)00303-3), 1997.
- 769 Stiegler, C., Koebisch, F., Ali, A. A., June, T., Veldkamp, E., Corre, M. D., Koks, J., Tjoa, A., Knohl, A.:
770 Temporal variation in nitrous oxide (N₂O) fluxes from an oil palm plantation in Indonesia: An
771 ecosystem-scale analysis, *GCB Bioenergy*, 15, 1221–39, <https://doi.org/10.1111/gcbb.13088>,
772 2023.
- 773 The, Y. A., Silver, W. L., Conrad, M. E.: Oxygen effects on methane production and oxidation in humid
774 tropical forest soils, *Glob. Chang. Biol.*, 11, 1283–1297, [https://doi.org/10.1111/j.1365-](https://doi.org/10.1111/j.1365-2486.2005.00983.x)
775 2486.2005.00983.x, 2005.
- 776 The, Y. A., Silver, W. L.: Effects of soil structure destruction on methane production and carbon



- 777 partitioning between methanogenic pathways in tropical rain forest soils, *J. Geophys. Res. G:*
778 *Biogeosciences*, 111, G1, <https://doi.org/10.1029/2005JG000020>, 2006.
- 779 Tian, H., Chen, G., Lu, C., Xu, X., Ren, W., Zhang, B., Banger, K., Tao, B., Pan, S., Liu, M., Zhang, C.: Global
780 methane and nitrous oxide emissions from terrestrial ecosystems due to multiple environmental
781 changes, *Ecosyst. Health Sustain.*, 1, 1–20, <https://doi.org/10.1890/EHS14-0015.1>, 2015.
- 782 Van Langenhove, L., Verryckt, L. T., Bréchet, L., Courtois, E. A., Stahl, C., Hofhansl, F., Bauters, M.,
783 Sardans, J., Boeckx, P., Fransen, E., Peñuelas, J.: Atmospheric deposition of elements and its
784 relevance for nutrient budgets of tropical forests, *Biogeochemistry*, 149, 175–93,
785 <https://doi.org/10.1007/s10533-020-00673-8>, 2020.
- 786 Wagner, F., Hérault, B., Stahl, C., Bonal, D., Rossi, V.: Modeling water availability for trees in tropical
787 forests, *Agric. For. Meteorol.*, 151, 1202–13, <https://doi.org/10.1016/j.agrformet.2011.04.012>,
788 2011.
- 789 Wang, Z. P., Chang, S. X., Chen, H., Han, X. G.: Widespread non-microbial methane production by
790 organic compounds and the impact of environmental stresses, *Earth-Sci. Rev.*, 127, 193–202,
791 <https://doi.org/10.1016/j.fuel.2015.12.074>, 2013.
- 792 Wang, H., Li, H., Liu, Z., Lv, J., Song, X., Li, Q., Jiang, H., Peng, C.: Observed methane uptake and
793 emissions at the ecosystem scale and environmental controls in a subtropical forest, *Land*, 10,
794 975, <https://doi.org/10.3390/land10090975>, 2021.
- 795 Welch, B., Gauci, V., Sayer, E. J.: Tree stem bases are sources of CH₄ and N₂O in a tropical forest on
796 upland soil during the dry to wet season transition, *Glob. Chang. Biol.*, 25, 361–72,
797 <https://doi.org/10.1111/gcb.14498>, 2019.
- 798 Werner, C., Zheng, X., Tang, J., Xie, B., Liu, C., Kiese, R., Butterbach-Bahl, K.: N₂O, CH₄ and CO₂ emissions
799 from seasonal tropical rainforests and a rubber plantation in Southwest China, *Plant Soil*, 289,
800 335–53, <https://doi.org/10.1007/s11104-006-9143-y>, 2006.
- 801 Werner, C., Kiese, R., Butterbach-Bahl, K.: Soil-atmosphere exchange of N₂O, CH₄, and CO₂ and
802 controlling environmental factors for tropical rain forest sites in western Kenya, *J. Geophys. Res.-*



- 803 Atmos., 112, D3, <https://doi.org/10.1029/2006JD007388>, 2007.
- 804 Wickham, H., Wickham, H.: Getting Started with ggplot2. ggplot2: Elegant graphics for data analysis,
805 11–31, 2016.
- 806 Whiting, G. J., Chanton, J. P.: Primary production control of methane emission from wetlands, Nature,
807 364, 794–5, <https://doi.org/10.1038/364794a0>, 1993.
- 808 Wright, E. L., Black, C. R., Cheesman, A. W., Drage, T., Large, D., Turner, B. L., Sjoegersten, S.:
809 Contribution of subsurface peat to CO₂ and CH₄ fluxes in a neotropical peatland, Glob. Chang.
810 Biol., 17, 2867–81, <https://doi.org/10.1111/j.1365-2486.2011.02448.x>, 2011.
- 811 Wood, S., Wood, M. S.: Package “mgcv”. R package version, 1:729, 2015.
- 812 Wood, S. N.: Generalized additive models: an introduction with R. chapman and hall/CRC, Boca Raton.,
813 Pp 496, <https://doi.org/10.1201/9781315370279>, 2017.
- 814 Yu, L., Zhu, J., Ji, H., Bai, X., Lin, Y., Zhang, Y., Sha, L., Liu, Y., Song, Q., Dörsch, P., Mulder, J.: Topography-
815 related controls on N₂O emission and CH₄ uptake in a tropical rainforest catchment, Sci. Total
816 Environ., 775, 145616, <https://doi.org/10.1016/j.scitotenv.2021.145616>, 2021.
- 817 Zhu, J., Mulder, J., Wu, L.P., Meng, X. X., Wang, Y. H., Dörsch, P.: Spatial and temporal variability of N₂O
818 emissions in a subtropical forest catchment in China, Biogeosciences, 10, 1309–21,
819 <https://doi.org/10.5194/bg-10-1309-2013>, 2013.